

Neuron

A Critical Period for Experience-Dependent Remodeling of Adult-Born Neuron Connectivity

Highlights

- An enriched environment (EE) alters adult-born neuron presynaptic connectivity
- EE-induced input remodeling is restricted to a critical period
- Inputs from interneurons are differentially affected by EE and running
- Cortical innervation remains stable following return to impoverished housing

Authors

Matteo Bergami,
Giacomo Masserdotti, ...,
Magdalena Götz, Benedikt Berninger

Correspondence

matteo.bergami@uk-koeln.de

In Brief

Bergami et al. utilize a monosynaptic tracing technique to demonstrate that the circuit incorporation of adult-born hippocampal neurons is not prefigured, but regulated by experience. This connectivity remodeling entails changes in local and long-range inputs that are differentially stabilized over time.



A Critical Period for Experience-Dependent Remodeling of Adult-Born Neuron Connectivity

Matteo Bergami,^{1,2,*} Giacomo Masserdotti,^{2,3} Silvio G. Temprana,⁴ Elisa Motori,⁵ Therese M. Eriksson,¹ Jana Göbel,¹ Sung Min Yang,⁴ Karl-Klaus Conzelmann,⁶ Alejandro F. Schinder,⁴ Magdalena Götz,^{2,3,7} and Benedikt Berninger^{2,8,9}

¹Cologne Excellence Cluster on Cellular Stress Responses in Aging-Associated Diseases (CECAD) and University Hospital of Cologne, 50931 Cologne, Germany

²Physiological Genomics, Institute of Physiology, Ludwig Maximilians University Munich, 80336 Munich, Germany

³Institute of Stem Cell Research, Helmholtz Zentrum München, 85764 Neuherberg, Germany

⁴Laboratory of Neuronal Plasticity, Leloir Institute (IIBBA, CONICET), C1405BWE Buenos Aires, Argentina

⁵Department of Mitochondrial Biology, Max Planck Institute for Biology of Ageing, 50931 Cologne, Germany

⁶Max von Pettenkofer Institute and Gene Center, Ludwig Maximilians-University Munich, 81377 Munich, Germany

⁷Munich Cluster for Systems Neurology (SyNergy), 80336 Munich, Germany

⁸Institute of Physiological Chemistry, University Medical Center of the Johannes Gutenberg University, 55128 Mainz, Germany

⁹Focus Program Translational Neuroscience, Johannes Gutenberg University, 55131 Mainz, Germany

*Correspondence: matteo.bergami@uk-koeln.de

<http://dx.doi.org/10.1016/j.neuron.2015.01.001>

SUMMARY

Neurogenesis in the dentate gyrus (DG) of the adult hippocampus is a process regulated by experience. To understand whether experience also modifies the connectivity of new neurons, we systematically investigated changes in their innervation following environmental enrichment (EE). We found that EE exposure between 2–6 weeks following neuron birth, rather than merely increasing the number of new neurons, profoundly affected their pattern of monosynaptic inputs. Both local innervation by interneurons and to even greater degree long-distance innervation by cortical neurons were markedly enhanced. Furthermore, following EE, new neurons received inputs from CA3 and CA1 inhibitory neurons that were rarely observed under control conditions. While EE-induced changes in inhibitory innervation were largely transient, cortical innervation remained increased after returning animals to control conditions. Our findings demonstrate an unprecedented experience-dependent reorganization of connections impinging onto adult-born neurons, which is likely to have important impact on their contribution to hippocampal information processing.

INTRODUCTION

Newly generated neurons in the adult dentate gyrus (DG) contribute uniquely to hippocampal information processing (Marín-Burgin et al., 2012; Nakashiba et al., 2012), which becomes manifest on the behavioral level by the fact that specific loss of adult-generated neurons or major changes in their number can alter memory performances, stress responses, and explorative activity (Bergami et al., 2008; Freund et al., 2013; Sa-

hay et al., 2011; Saxe et al., 2006; Snyder et al., 2011). It is believed that the unique functional contribution of these neurons depends on their heightened electrical excitability facilitating neuronal spiking in response to excitatory input (Mongiat et al., 2009; Schmidt-Hieber et al., 2004), as well as on their increased synaptic plasticity (Ge et al., 2007; Schmidt-Hieber et al., 2004) during a narrow time window following a neuron's birth coined the critical period. While early (N-methyl-D-aspartate) (NMDA) receptor activation is important for the survival of adult-generated neurons (Tashiro et al., 2006), increased excitability favors the preferential recruitment of new neurons into active hippocampal memory circuits (Kee et al., 2007; Marín-Burgin et al., 2012), and enhanced long-term potentiation mediated by NR2B-containing NMDA receptors at 4–6 weeks of neuron age (Ge et al., 2007) appears to be crucial for the functional contribution of adult-generated neurons to context discrimination (Kheirbek et al., 2012b), underscoring the importance of the critical period for the functional integration of adult-generated neurons in the DG.

Very little is known about how the connectivity pattern of adult-generated neurons develops during their own ontogeny and how this is modified by experience, particularly during the critical period. Indeed, it is very likely that the state of connectivity is of similar importance for the functional contribution of adult-generated neurons to network activity as are their well-known characteristic cell-intrinsic properties of heightened excitability and synaptic plasticity.

In the DG, a temporal sequence of presynaptic innervation onto adult-generated neurons, at first by local interneurons, then followed later by subcortical and finally cortical projection neurons, results in a stepwise integration into the pre-existing network (Deshpande et al., 2013; Espósito et al., 2005; Vivar et al., 2012). An intriguing aspect of this integration process is that the extent of neurons added to the network can be modulated by experiences such as exposure to an enriched environment (EE) and voluntary exercise (Kempermann et al., 1997; van Praag et al., 1999). While merely increasing the number of newly added neurons may improve hippocampal information

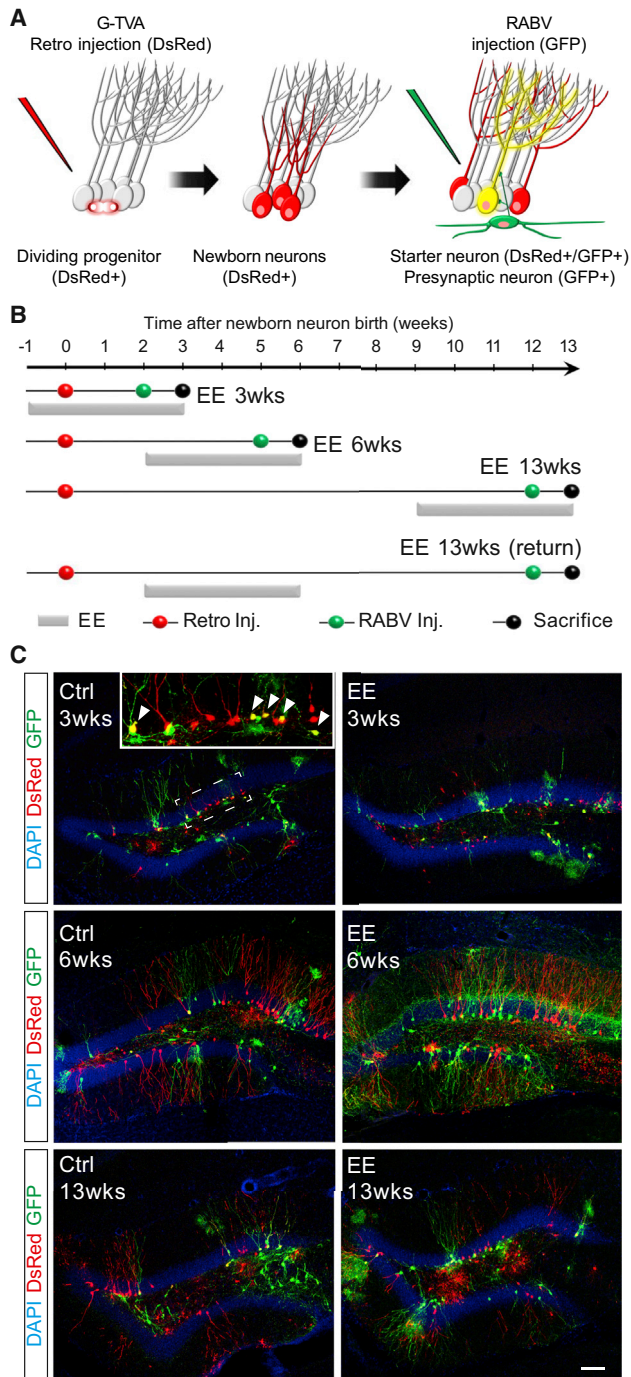


Figure 1. RABV-Mediated Tracing of Newborn Neuron Inputs

(A) Experimental design for tracing monosynaptic connections impinging onto adult-born neurons via consecutive delivery of G and TVA-expressing retrovirus and RABV.

(B) Timeline of the experimental protocols (EE 3 weeks, EE 6 weeks, EE 13 weeks, and EE 13 weeks, return). Periods of continuous EE are indicated with gray bars.

(C) Examples of local tracing obtained following EE 3 weeks, EE 6 weeks, EE 13 weeks, and corresponding controls. Arrowheads in the inset point to double transduced newborn starter neurons.

Scale bar represents 70 μm . See also [Figures S1](#) and [S2](#).

processing capacity and thereby exert beneficial effects on cognition and affective disorders ([Aimone et al., 2011](#); [Kheirbek et al., 2012a](#)), it has remained entirely elusive whether experience also affects the establishment of new neurons' connectivity. Here, by taking advantage of a previously validated rabies virus (RABV)-based monosynaptic tracing technique ([Wickersham et al., 2007](#)), we report a surprising degree of circuit remodeling in response to EE, which links for the first time experience to ontogenetic stage-restricted changes in newborn neurons' presynaptic input.

RESULTS

After having confirmed that neuronal activity does not directly affect the transsynaptic spread of RABV (see [Supplemental Experimental Procedures](#) and [Figure S1](#) available online) ([Ugolini, 2011](#)), thus validating a dual virus-based monosynaptic tracing technique for detecting changes in connectivity patterns ([Deshpande et al., 2013](#); [Li et al., 2013](#); [Vivar et al., 2012](#)), we exposed adult mice to a 4-week-long period of EE ([Figure S2A](#)) and examined the resulting alterations in the spectrum of presynaptic inputs impinging onto adult-generated DG granule neurons. To this end, a GFP-encoding, EnvA-pseudotyped ΔG RABV ([Wickersham et al., 2007](#)) was delivered to the DG of adult mice at different times following infection with a G-TVA retrovirus encoding (1) the EnvA receptor (TVA) for restricting primary RABV infection to newborn neurons as "starter" population and (2) the RABV glycoprotein (G), which is necessary for subsequent monosynaptic transfer (via transcomplementation) to their first-order presynaptic partners ([Figure 1A](#)).

As EE may have distinct effects on new neurons' survival ([Tashiro et al., 2007](#)) and synaptic integration according to their stage of maturation, we designed an experimental protocol of exposing neurons to EE at different times following their birth ([Figure 1B](#)): during their first 3 weeks of life (EE 3 weeks), between weeks 2 and 6 after their birth (EE 6 weeks), and between weeks 9 and 13 (EE 13 weeks). Starter cells were transduced with RABV 1 week prior to sacrifice and sections analyzed for reporter double-positive (DsRed+/GFP+) starter neurons ([Figure S2B](#)) and GFP-only positive first-order presynaptic partner neurons ([Figure 1C](#)). Based on their anatomical localization, morphology, and marker expression ([Deshpande et al., 2013](#)), the type of GFP-only positive presynaptic neurons within the DG were identified as glutamatergic hilar mossy cells or distinct types of GABAergic interneurons distributed between the hilus (e.g., HIPP cells), the subgranular zone (SGZ)/granule cell layer (GCL) (e.g., basket cells and hilar commissural-associational pathway-related cells [HICAP] cells) and the molecular layer (ML; e.g., MOPP and axo-axonic cells) ([Figure 2A](#)). We also observed occasional labeling of mature granule neurons, which, however, declined with increasing intervals between retrovirus and RABV infection, suggesting that this labeling is due to pseudotransduction of mature granule neurons as argued previously ([Deshpande et al., 2013](#)). EE exposure starting 1 week before and continuing for the entire first 3 weeks following new neurons' birth (EE 3 weeks) did not produce overt changes in their local connectivity as revealed by RABV tracing in comparison to non-enriched animals ([Figures 1C](#) and [2B](#)). Likewise, the number of

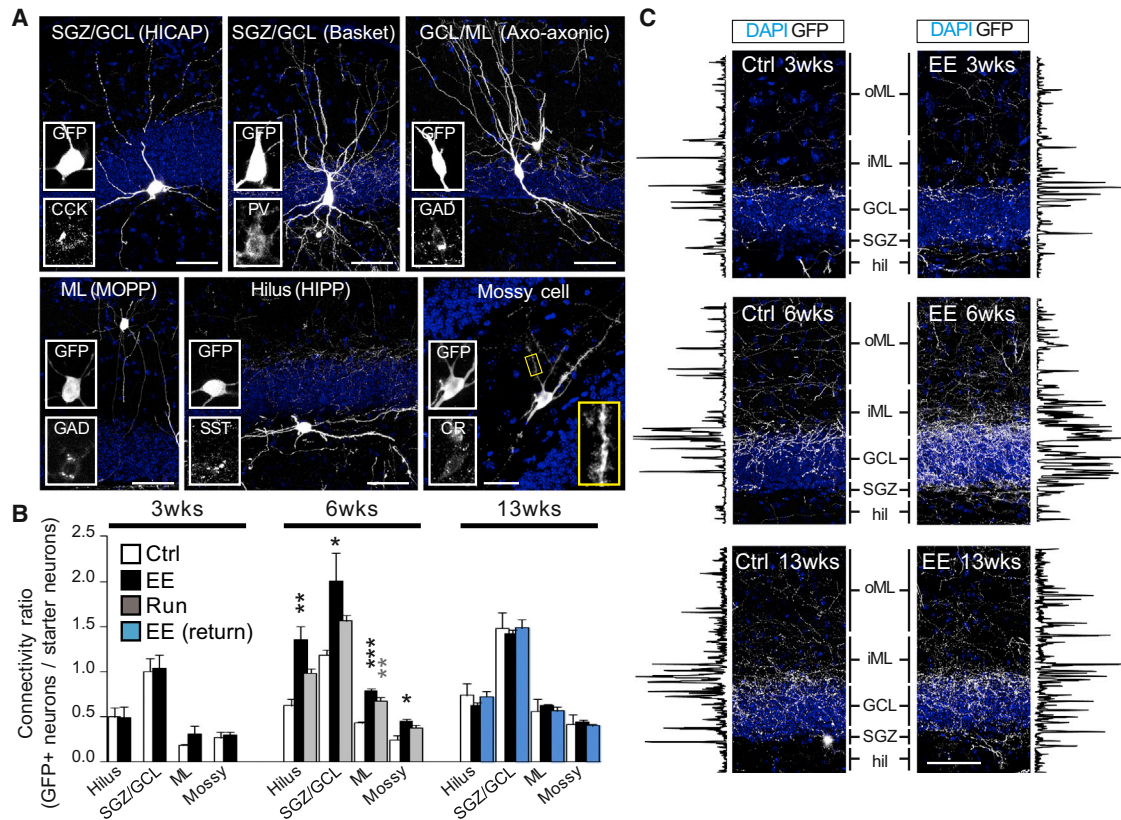


Figure 2. Experience-Dependent Changes of New Neuron Local Connectivity

(A) Examples of traced presynaptic neurons local to newborn DG neurons. Traced neurons were classified according to their morphology and position within the DG. Insets depict high magnifications of the cell body and the corresponding immunoreactivity for the indicated markers. Scale bars represent 30 μ m.

(B) Quantification of presynaptic connectivity ratio (GFP+ presynaptic neurons normalized on GFP+/DsRed+ starter neurons) performed at the indicated times following retroviral labeling and after control housing (Ctrl), enrichment (EE), running (Run), and returning EE-exposed animals to control housing (EE return) ($n = 3-5$ mice per group, * $p < 0.05$, ** $p < 0.01$, *** $p < 0.001$; data are represented as mean \pm SEM).

(C) Photomicrographs depicting the density of presynaptic axonal fibers innervating the DG. Line-scan analysis on each side shows layer-specific densities of presynaptic fibers. oML, outer molecular layer; iML, inner molecular layer; hil, hilus.

Scale bar represents 50 μ m. See also Figure S2.

labeled presynaptic cells was similar for control and EE-exposed mice following EE 13 weeks (Figures 1C and 2B). In contrast, a significantly higher proportion (about 2-fold) of all classes of presynaptic local interneurons was detected, when EE was provided between the second and sixth week of the neurons' life (Figures 1C and 2B). These changes were mirrored by a sharp increase in the amount of GFP+ axonal fibers within the DG, which profusely innervated the SGZ, GCL, and inner portions of the ML (Figure 2C). Most of these axon terminals originated from the aforementioned local interneurons; however, part of the axon collaterals invaded the DG from adjacent hippocampal structures.

Intriguingly, following EE 6 weeks, a considerable amount of GFP+ presynaptic neurons was found within the CA1 and CA3 subfields of the hippocampus (Figures 3A and 3B), projecting to the DG. These neurons were distributed throughout the CA hippocampal subfields, yet with the exception of occasional CA3 pyramidal cells (Vivar et al., 2012) (Figure S3A), their position, marker expression, and morphology were characteristic of interneurons (Freund and Buzsáki, 1996) (Figures 3C and S3B–

S3E). The majority of the GFP+ neurons and their smooth dendritic arbors were located in stratum oriens, often bordering with the alveus (Figures 3B and 3C). The remaining of the labeled interneurons was found in the strata lacunosum moleculare, radiatum, and lucidum/pyramidale (Figures 3C, 3D, and S3B–S3D). While some classes of interneurons have been previously described to directly project to the DG by crossing the hippocampal fissure (Klausberger and Somogyi, 2008; Sik et al., 1994), these neurons were only sporadically labeled in nonenriched animals or following EE 3 weeks and 13 weeks (at about 6- to 13-fold lower frequency in controls compared with EE 6 weeks; Figure 3D). Of note, a conspicuous number of GFP+ projection neurons were also found in the subiculum (Deshpande et al., 2013) (Figure S3D). Intriguingly, voluntary exercise between weeks 2 and 6 (Run 6 weeks) alone, while known to enhance neurogenesis similar to EE (van Praag et al., 1999), elicited only a modest change in inputs arising from hippocampal interneurons (Figures 2B, 3B, and 3D), suggesting for a specific effect of EE on local innervation and cross-regional inhibitory feedback onto newborn neurons during a defined period of synaptic integration.

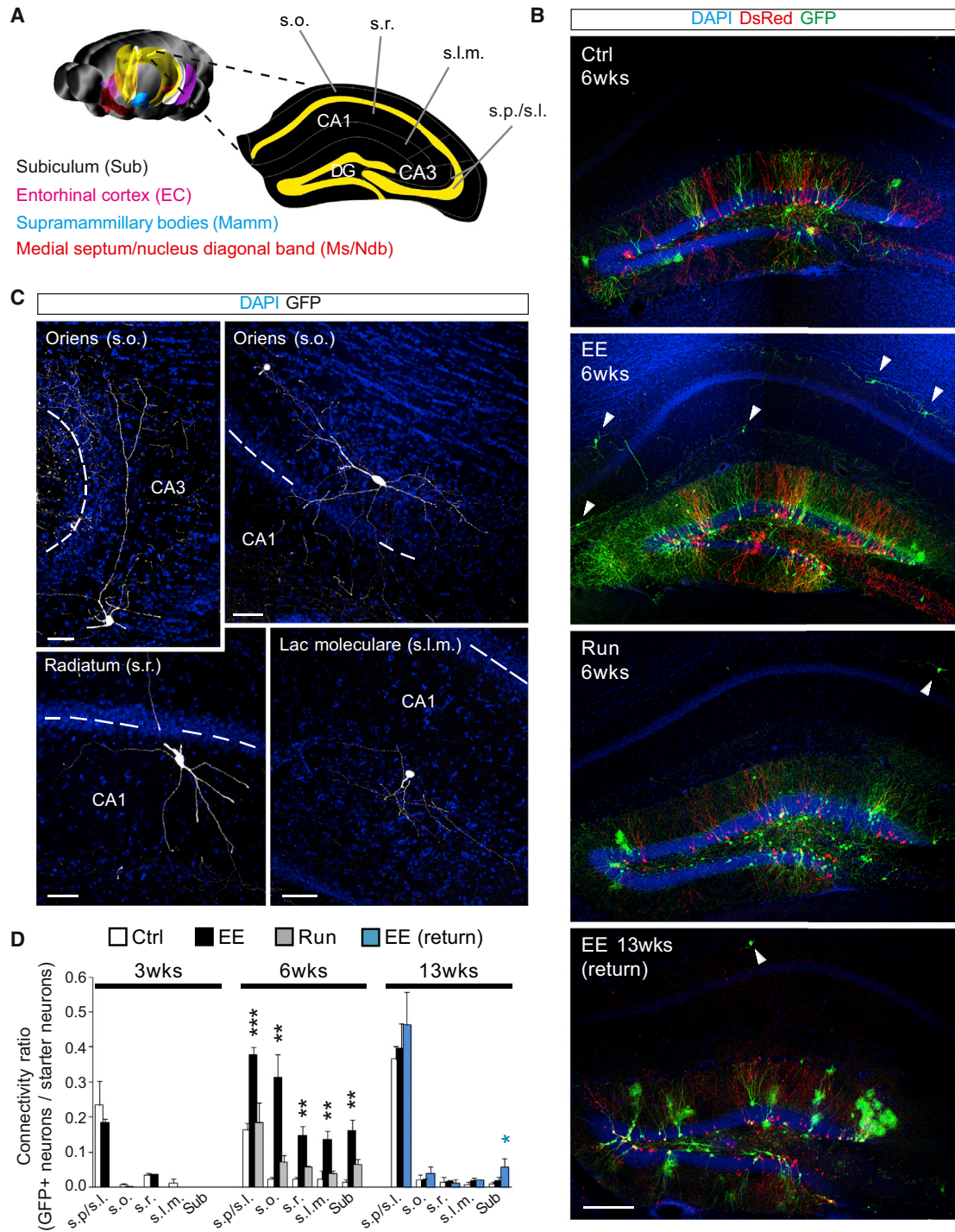


Figure 3. Experience-Dependent Remodeling of Hippocampal Projections to Newborn Neurons

(A) Scheme showing the hippocampal layers and the other extrahippocampal regions in which traced neurons were found (s.o., stratum oriens; s.p./s.l., stratum pyramidale/lucidum; s.r., stratum radiatum; s.l.m., stratum lacunosum moleculare).

(B) Examples taken from control, EE-exposed, and running (Run) mice at the indicated times showing the distribution of hippocampal presynaptic neurons (arrowheads). Scale bar represents 130 μ m.

(C) Examples of traced interneurons in the CA1 and CA3 subfields. Dashed line indicates the pyramidal layer. Scale bars represent 40 μ m.

(D) Quantification of hippocampal connectivity ratio in control, enriched, and running animals at the indicated times (n = 3–5 mice per group, *p < 0.05, **p < 0.01, ***p < 0.001; data are represented as mean \pm SEM).

See also Figure S3.

Next, we examined the innervation by long-range projection neurons of subcortical and cortical origins previously shown to impinge onto adult-born hippocampal neurons (Deshpande et al., 2013; Vivar et al., 2012). With the exception of neurons located in the mammillary bodies (Mamm), whose small proportion remained overall stable between all the experimental paradigms, the number of labeled cholinergic neurons located in the medial septum/nucleus of diagonal band of Broca (Ms/Ndb) and in particular that of projection neurons within the lateral EC steadily increased over time in nonenriched animals (Figure 4A). Strikingly, however, following both EE 6 weeks and Run 6 weeks, but not upon EE 3 weeks and 13 weeks, the number of GFP+ neurons dramatically increased in Ms/Ndb and EC (Figures 4A, 4B, S4A, and S4B). These data show that like local inputs, long-range projections are selectively increased in number following exposure to EE during a specific time window, but also provide evidence for differential regulation of local and long-range connection in response to running. In order to subject the finding that EE can modify the extent of cortical innervation to an independent experimental test, we measured the density of mushroom spines in newly generated DG neurons at 6 and 13 weeks after their generation (EE 6 weeks and 13 weeks). EE 6 weeks produced a 2- to 3-fold increase in overall mushroom spine density compared with control conditions (Figures 4C and 4D), irrespective of the position along the dendritic shaft and the location of the neuron along the septo-temporal axis of the hippocampus (Figures 4E–4G). These data show that 4 weeks of EE can induce structural rearrangements in the dendritic innervation of adult-born neurons, thus independently corroborating the increase in EC innervation observed by RABV tracing. In contrast, EE 13 weeks did not elicit any significant changes in mushroom spine density compared with controls (Figures 4C and 4D), again arguing in favor of a restricted period of enhanced structural plasticity in new neurons between weeks 2 and 6 after their generation. Overall, during a specific period, EE produced significant changes in the presynaptic connectivity of new neurons comprising a 1.8 ± 0.3 -fold increase in local inputs, a 4.1 ± 0.8 -fold increase in hippocampal inputs, and a 4.1 ± 0.7 -fold increase in long-range cortical and subcortical inputs (Figure 4H). Intriguingly, patch-clamp recordings from hippocampal slices of control and EE 6-week-exposed animals revealed a reduction in the ratio between excitation and inhibition as evidenced by the frequency of spontaneous excitatory and inhibitory synaptic currents (Figures S4E–S4G), which indicates additional layers of regulation by EE 6 weeks on the synaptic level.

Finally, we asked the question to which extent the enhancement of local and long-range connectivity induced by EE 6 weeks remained stable following the return of animals to control housing conditions for additional 7 weeks (EE 13 weeks—return; Figure 1B). Notably, the pattern of innervation of newborn neurons by hippocampal interneurons (both of local origin or arising from interneurons in the CA subfields) was virtually indistinguishable from controls of the same age, suggesting that the changes in intrahippocampal connectivity required active maintenance and became reversed following environmental impoverishment (Figures 2B and 3D). In sharp contrast, the increase in cortical innervation as well as mushroom spine density induced during

EE 6 weeks remained stable even after returning mice to standard cages (Figures 4A–4D). These data indicate that some changes in connectivity, presumably via pruning mechanisms, can still occur after the end of the critical period, yet innervation from the EC, once established, appears to be robust against experience-dependent changes after closure of the critical window.

DISCUSSION

In this study we provide evidence for an experience-dependent reorganization of the presynaptic connectivity of adult-generated DG granule neurons, as evidenced by quantitative and qualitative alterations in the labeling of presynaptic partners using a RABV-based tracing technique. Several lines of control experiments (Figure S1) corroborate that the alterations in tracing were not due to activity-dependent changes in RABV biosynthesis and transsynaptic spread itself. Thus, the data presented here provide evidence for true structural plasticity and demonstrate that important changes in network connectivity can occur within a specific time window during the maturation of newly generated neurons (2–6 weeks of age; Figure 1B). This time window coincides with the well-known critical period of enhanced synaptic plasticity previously described (Ge et al., 2007; Kheirbek et al., 2012b), suggesting that synaptic plasticity mechanisms may contribute to the establishment and stabilization of the presynaptic innervation pattern (Chancey et al., 2013). While the increase in local and long-range connectivity was restricted to a critical time window of 2–6 weeks following neuron birth, intrahippocampal connections appeared to be still capable of undergoing refinement, as evidenced by the decline in most of the local connectivity upon returning the animals from EE to control conditions, indicating some degree of plasticity still beyond the critical period. Of note, in controls, connections arising from interneurons in the stratum pyramidale and stratum lucidum had increased by 13 weeks to a similar level as reached following EE 6 weeks, suggesting that exposure to EE may have accelerated the establishment of this source of inhibitory input. It is tempting to speculate that the dynamic turnover of inhibitory synaptic contacts onto new neurons contributes to shaping the window of the critical period and thus sculpting the final connectivity of adult-generated neurons. In contrast to local innervation, the tracing of cortical inputs remained unaffected by the return to standard housing, arguing for a more stable nature of these connections once they have been established. This stability may reflect the establishment of specific information channels by mapping specific EC inputs onto particular newborn granule neurons during the critical period as hypothesized previously (Bergami and Berninger, 2012).

Besides revealing canonical connections onto adult-generated neurons, RABV tracing of EE-exposed mice also disclosed a previously unknown source of input arising from interneurons of the CA3 and CA1 subfields. This set of connections was virtually undetectable under control conditions, suggesting that during basal levels of network activity, they may exert little regulatory influence on the activity of adult-generated neurons, but became manifest following EE 6 weeks, embedding adult-generated neurons into a novel feedback inhibitory circuitry. Given that EE represents a more physiological condition than standard

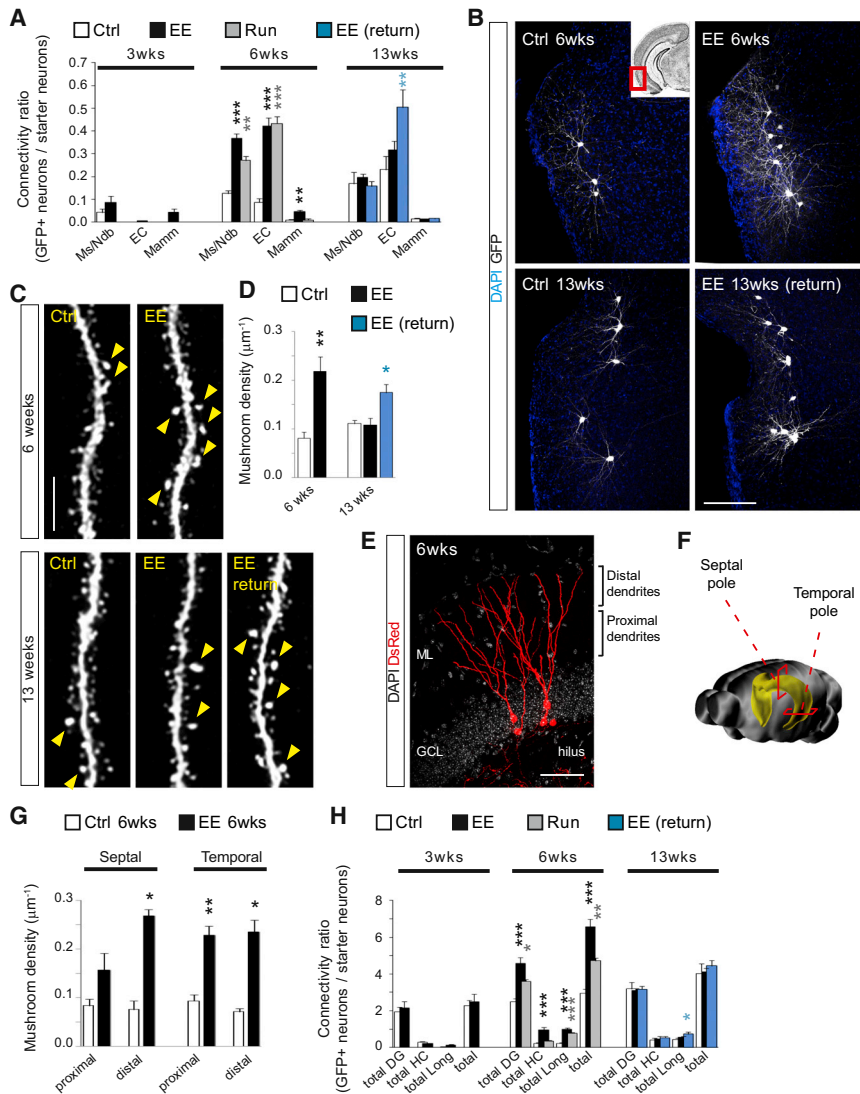


Figure 4. Subcortical/Cortical Innervation and Spine Growth in Adult-Born Neurons following EE

(A) Quantification of long-range projection neurons in subcortical and cortical areas ($n = 3-5$ mice per group, * $p < 0.05$, ** $p < 0.01$, *** $p < 0.001$; data are represented as mean \pm SEM). Ms/Ndb, medial septum and nucleus diagonal band of Broca; EC, entorhinal cortex; Mamm, mammillary bodies.

(B) Examples of RABV-traced projection neurons in the entorhinal cortex of control mice and following EE (6 wks and 13 wks return paradigms). Inset shows the location of traced neurons. Scale bar represents 100 μ m.

(C) Examples of dendritic segments taken at 6 and 13 weeks after retroviral labeling of control and EE-exposed newborn neurons. Arrowheads point to mushroom spines (spine area $\geq 0.4 \mu$ m²). Scale bar represents 5 μ m.

(D) Density of mushroom spines in control neurons and following EE 6 weeks, EE 13 weeks, and EE 13 weeks-return paradigms ($n = 3-4$ mice per group, * $p < 0.05$, ** $p < 0.01$; data are represented as mean \pm SEM).

(E) Photomicrograph of 6-week-old newborn neurons expressing DsRedExpress2 and the subdivision of their dendrites into proximal (inner and middle third of the ML) and distal (outer third of the ML). Scale bar represents 50 μ m.

(F) Scheme showing the distinction between septal and temporal poles of the hippocampus.

(G) Density of mushroom spines in 6-week-old control and EE-exposed newborn neurons ($n = 3$ mice per group, * $p < 0.05$, ** $p < 0.01$; data are represented as mean \pm SEM).

(H) Quantification of newborn neuron connectivity ratio divided among local (DG), hippocampal (HC), and cortical/subcortical (Long) regions ($n = 3-5$ mice per group; * $p < 0.05$, ** $p < 0.01$; *** $p < 0.001$; data are represented as mean \pm SEM). See also Figure S4.

housing, this feedback inhibitory circuit may be functionally important in facilitating the sparse activation of newborn neurons by cortical inputs (hence favoring pattern separation) and modulating the way spatial information is conveyed to the downstream CA3 region (Aimone et al., 2011; Dieni et al., 2013; Ikrar et al., 2013; Klausberger and Somogyi, 2008). Alternatively, the fact that these inhibitory connections appear mostly transient in nature might suggest that they play a specific role in the regulation of excitatory cortical inputs during activity-dependent synaptic refinement.

Our findings also demonstrate the existence of a more complex effect of EE and voluntary exercise than the previously described mere increase in newborn neuron numbers, which has been correlated with the amelioration of cognitive abilities and anxiety- and depression-related behaviors (van Praag et al., 2000). In fact, while genetic manipulations aimed at increasing adult neurogenesis are sufficient to improve pattern separation, they only reproduce the behavioral response of antidepressants when coupled to voluntary exercise (Sahay et al.,

2011). One may therefore hypothesize that some of the anxiolytic effects produced by exercise and EE, rather than depending on the simple addition of more neurons, require a functional reorganization of the synaptic circuitry during newborn neurons' incorporation. Of note, exercise and EE differentially affected presynaptic connectivity of newborn neurons. For instance, while cortical innervation was increased similar to EE following voluntary running (Figure 4A), local and hippocampal connectivity were only slightly modified (Figures 2B and 3D). These differences in circuit remodeling reveal paradigm-specific effects on the connectivity of newborn neurons well in line with the differential behavioral consequences observed after EE and running (Clemenson et al., 2014).

Intriguingly, the overall excitation/inhibition balance of synaptic inputs in EE-exposed new neurons (6-week paradigm) was decreased compared with control neurons (Figures S4E–S4G), hinting at a dissociation of spine density and frequency of excitatory synaptic input. This may reflect additional, potentially homeostatic, changes in the quality of synaptic transmission,

such as reduced release probability at excitatory synapses (given the lack of changes in synaptic current amplitude and the apparent increase in the number of synaptic connections as revealed by monosynaptic tracing). These changes in excitation/inhibition balance may result in a reduced activation of neurons exposed to EE, which suggests an accelerated acquisition of more mature functional properties (Marín-Burgin et al., 2012).

In conclusion, understanding the functional implications of the experience-dependent remodeling of presynaptic connectivity described here may provide fundamental new insights into the unique contribution of adult-born neurons to information processing and how environmental factors can result in the emergence of individual differences in brain plasticity and emotional behavior (Freund et al., 2013).

EXPERIMENTAL PROCEDURES

Mice and Stereotactic Injections

Eight- to 10-week-old C57BL/6 mice were housed in groups of three to four. Housing conditions included nesting and bedding material, standard pellet food, and water provided ad libitum, 12 hr light and dark cycle, temperature of 21°C–22°C and cage replacement once per week. EE was provided for 4 consecutive weeks by housing mice in larger cages (about 100 × 50 cm) equipped with paper tunnels, colored plastic tunnels and other toys, nesting material, and running wheels. For surgery, mice were anesthetized via an intraperitoneal injection of midazolam (5 mg per kg of body weight), medetomidine (0.5 mg per kg), and fentanyl (0.05 mg per kg) and placed in a stereotactic apparatus. A small craniotomy was performed, and ~0.5 μ l of retrovirus or ~0.2 μ l RABV was slowly injected in the dorsal DG (relative to Bregma: caudal 2.0, lateral 1.6, and ventral 1.8–2.0) during a time window of 10–20 min, by using a finely pulled capillary connected to a pulse generator (WPI). After infusion, the capillary was left in place for additional 10 min to allow complete diffusion of the virus. The skin incision was closed carefully after retroviral injection to minimize inflammation and in order to facilitate the subsequent RABV injection. After surgery, anesthesia was antagonized with an intraperitoneal injection of atipamezol (2.5 mg per kg), flumazenil (0.5 mg per kg), and naloxone (1.2 mg per kg). Animals were allowed to recover, and physical conditions were monitored daily to improve their welfare before euthanizing them. All animal procedures were performed in agreement with the European Union and German guidelines and were approved by the Government of State of Upper Bavaria.

Viral Vectors

The retroviral constructs used in this study were derived from a Moloney Murine Leukemia Virus-based retroviral vector in which gene expression is driven by the chicken beta-actin promoter (van Praag et al., 2002) (CAG). The retrovirus encoding for *DsRedExpress2*, the RABV glycoprotein (G) and the *TVA800* (the GPI anchored form of the TVA receptor), designed as CAG-*DsRedExpress2-2A-G-IRES2-TVA* (i.e., G-TVA retrovirus), was described previously (Deshpande et al., 2013). Retroviral plasmid was used to transfect the helper-free HEK293 gpg cell line using Lipofectamine 2000T, and virus was harvested at 2, 4, and 6 days after transfection, followed by ultracentrifugation. Titers used for experiments were typically in the range of $5 - 9 \times 10^7$. Construction of the G gene-deleted GFP-expressing RABV (SAD Δ G-GFP) has been described before (Wickersham et al., 2007). The RABV SAD Δ G-GFP was amplified in BSR MG-on cells complementing the G deficiency of the virus upon induction of G expression by doxycyclin as previously described (Finke et al., 2003). Pseudotyping of SAD Δ G-GFP with EnvA was performed by infection of BHK-EnvARGCD cells, expressing an ASLV-A envelope protein comprising the RABV G cytoplasmic tail at a multiplicity of infection of 1 as described previously (Wickersham et al., 2007).

Imaging and Quantitative Analysis

Samples were imaged with a confocal laser-scanning microscope (LSM 710, Zeiss) equipped with four laser lines (405, 488, 561, and 633 nm) and

10 \times (NA 0.3), 25 \times (NA 0.8), 40 \times (NA 1.1), or 63 \times (NA 1.3) objectives. In alternative, a TCS SP8 Leica confocal system equipped with a white light laser was used. Quantifications were performed by counting the number of double-transduced (GFP+ and DsRed+) and RABV-only transduced cells (GFP+) per mouse (or culture). The number of RABV-only transduced cells was normalized on double-transduced cells to take into account for changes in the number of starter neurons. For quantification of mushroom spine density in labeled adult-born neurons, dendritic segments in the outer- and inner-medial ML of the septal and temporal hippocampal poles were randomly acquired at 80 \times or 100 \times , using an interstack interval of 0.3 μ m. Images were subsequently processed by deconvolution (Huygens Pro, Scientific Volume Imaging). Upon image calibration, ImageJ was used to manually quantify linear spine density and to estimate the individual cross-sectional area of relatively large spines (mushroom spines were classified having an area $\geq 0.4 \mu\text{m}^2$) (Zhao et al., 2006).

Statistical Analysis

Statistical analysis was obtained with GraphPad Prism 5 (GraphPad Software) using the Student's t test for comparisons between two datasets and one-way ANOVA followed by Dunnett's post hoc test for multiple group comparisons, unless otherwise indicated.

SUPPLEMENTAL INFORMATION

Supplemental Information includes Supplemental Experimental Procedures and four figures and can be found with this article online at <http://dx.doi.org/10.1016/j.neuron.2015.01.001>.

AUTHOR CONTRIBUTIONS

M.B. performed and analyzed most of the in vivo experiments. G.M. and K.-K.C. provided essential reagents. S.G.T., S.M.Y., and A.F.S. performed and analyzed electrophysiological recordings. E.M. performed in vitro experiments. T.M.E. and J.G. contributed to analysis. M.B., M.G., and B.B. developed the concept and designed experiments. M.B. and B.B. wrote the paper. All authors discussed and revised the manuscript.

ACKNOWLEDGMENTS

We thank Dr. A. Lepier and I. Muehlhahn (LMU Munich) for advice and help with virus preparation; Dr. M. Karow and E. Murenu (LMU Munich) for advice and help with the enrichment experiments; B. Fernando, N. Zapf, D. Franzen, and G. Jaeger for technical assistance; Dr. A. Schauss and the members of the CECAD imaging facility for assistance with microscopes. This work was supported by the LMU Research Fellowship program, a UoC Advanced Postdoctorate Grant, and Cologne Excellence Cluster on Cellular Stress Responses in Aging-Associated Diseases (CECAD) to M.B.; by the SFB870 (Deutsche Forschungsgemeinschaft) to K.-K.C. and M.G.; the Bundesministerium für Bildung und Forschung "Integration of stem cell-derived neurons" to B.B. and M.G.; the SFB1080 (Deutsche Forschungsgemeinschaft), the Belgian Science Policy Office (Wibrain) to B.B.; and the Howard Hughes Medical Institute (SIRS grant #55007652) and the Humboldt Foundation (Friedrich Wilhelm Bessel Research Award) to A.F.S.

Received: April 17, 2014

Revised: November 16, 2014

Accepted: December 24, 2014

Published: February 5, 2015

REFERENCES

- Aimone, J.B., Deng, W., and Gage, F.H. (2011). Resolving new memories: a critical look at the dentate gyrus, adult neurogenesis, and pattern separation. *Neuron* 70, 589–596.
- Bergami, M., and Berninger, B. (2012). A fight for survival: the challenges faced by a newborn neuron integrating in the adult hippocampus. *Dev. Neurobiol.* 72, 1016–1031.

- Bergami, M., Rimondini, R., Santi, S., Blum, R., Götz, M., and Canossa, M. (2008). Deletion of TrkB in adult progenitors alters newborn neuron integration into hippocampal circuits and increases anxiety-like behavior. *Proc. Natl. Acad. Sci. USA* *105*, 15570–15575.
- Chancey, J.H., Adlaf, E.W., Sapp, M.C., Pugh, P.C., Wadiche, J.I., and Overstreet-Wadiche, L.S. (2013). GABA depolarization is required for experience-dependent synapse unsilencing in adult-born neurons. *J. Neurosci.* *33*, 6614–6622.
- Clemenson, G.D., Lee, S.W., Deng, W., Barrera, V.R., Iwamoto, K.S., Fanselow, M.S., and Gage, F.H. (2014). Enrichment rescues contextual discrimination deficit associated with immediate shock. *Hippocampus*. Published online October 31, 2014. <http://dx.doi.org/10.1002/hipo.22380>.
- Deshpande, A., Bergami, M., Ghanem, A., Conzelmann, K.K., Lepier, A., Götz, M., and Berninger, B. (2013). Retrograde monosynaptic tracing reveals the temporal evolution of inputs onto new neurons in the adult dentate gyrus and olfactory bulb. *Proc. Natl. Acad. Sci. USA* *110*, E1152–E1161.
- Dieni, C.V., Nietz, A.K., Panichi, R., Wadiche, J.I., and Overstreet-Wadiche, L. (2013). Distinct determinants of sparse activation during granule cell maturation. *J. Neurosci.* *33*, 19131–19142.
- Espósito, M.S., Piatti, V.C., Laplagne, D.A., Morgenstern, N.A., Ferrari, C.C., Pitossi, F.J., and Schinder, A.F. (2005). Neuronal differentiation in the adult hippocampus recapitulates embryonic development. *J. Neurosci.* *25*, 10074–10086.
- Finke, S., Mueller-Waldeck, R., and Conzelmann, K.K. (2003). Rabies virus matrix protein regulates the balance of virus transcription and replication. *J. Gen. Virol.* *84*, 1613–1621.
- Freund, T.F., and Buzsáki, G. (1996). Interneurons of the hippocampus. *Hippocampus* *6*, 347–470.
- Freund, J., Brandmaier, A.M., Lewejohann, L., Kirste, I., Kritzler, M., Krüger, A., Sachser, N., Lindenberger, U., and Kempermann, G. (2013). Emergence of individuality in genetically identical mice. *Science* *340*, 756–759.
- Ge, S., Yang, C.H., Hsu, K.S., Ming, G.L., and Song, H. (2007). A critical period for enhanced synaptic plasticity in newly generated neurons of the adult brain. *Neuron* *54*, 559–566.
- Ikrar, T., Guo, N., He, K., Besnard, A., Levinson, S., Hill, A., Lee, H.K., Hen, R., Xu, X., and Sahay, A. (2013). Adult neurogenesis modifies excitability of the dentate gyrus. *Front. Neural Circuits* *7*, 204.
- Kee, N., Teixeira, C.M., Wang, A.H., and Frankland, P.W. (2007). Preferential incorporation of adult-generated granule cells into spatial memory networks in the dentate gyrus. *Nat. Neurosci.* *10*, 355–362.
- Kempermann, G., Kuhn, H.G., and Gage, F.H. (1997). More hippocampal neurons in adult mice living in an enriched environment. *Nature* *386*, 493–495.
- Kheirbek, M.A., Klemenhagen, K.C., Sahay, A., and Hen, R. (2012a). Neurogenesis and generalization: a new approach to stratify and treat anxiety disorders. *Nat. Neurosci.* *15*, 1613–1620.
- Kheirbek, M.A., Tannenholz, L., and Hen, R. (2012b). NR2B-dependent plasticity of adult-born granule cells is necessary for context discrimination. *J. Neurosci.* *32*, 8696–8702.
- Klausberger, T., and Somogyi, P. (2008). Neuronal diversity and temporal dynamics: the unity of hippocampal circuit operations. *Science* *321*, 53–57.
- Li, Y., Stam, F.J., Aimone, J.B., Goulding, M., Callaway, E.M., and Gage, F.H. (2013). Molecular layer perforant path-associated cells contribute to feed-forward inhibition in the adult dentate gyrus. *Proc. Natl. Acad. Sci. USA* *110*, 9106–9111.
- Marín-Burgin, A., Mongiat, L.A., Pardi, M.B., and Schinder, A.F. (2012). Unique processing during a period of high excitation/inhibition balance in adult-born neurons. *Science* *335*, 1238–1242.
- Mongiat, L.A., Espósito, M.S., Lombardi, G., and Schinder, A.F. (2009). Reliable activation of immature neurons in the adult hippocampus. *PLoS ONE* *4*, e5320.
- Nakashiba, T., Cushman, J.D., Pelkey, K.A., Renaudineau, S., Buhl, D.L., McHugh, T.J., Rodriguez Barrera, V., Chittajallu, R., Iwamoto, K.S., McBain, C.J., et al. (2012). Young dentate granule cells mediate pattern separation, whereas old granule cells facilitate pattern completion. *Cell* *149*, 188–201.
- Sahay, A., Scobie, K.N., Hill, A.S., O'Carroll, C.M., Kheirbek, M.A., Burghardt, N.S., Fenton, A.A., Dranovsky, A., and Hen, R. (2011). Increasing adult hippocampal neurogenesis is sufficient to improve pattern separation. *Nature* *472*, 466–470.
- Saxe, M.D., Battaglia, F., Wang, J.W., Malleret, G., David, D.J., Monckton, J.E., Garcia, A.D., Sofroniew, M.V., Kandel, E.R., Santarelli, L., et al. (2006). Ablation of hippocampal neurogenesis impairs contextual fear conditioning and synaptic plasticity in the dentate gyrus. *Proc. Natl. Acad. Sci. USA* *103*, 17501–17506.
- Schmidt-Hieber, C., Jonas, P., and Bischofberger, J. (2004). Enhanced synaptic plasticity in newly generated granule cells of the adult hippocampus. *Nature* *429*, 184–187.
- Sik, A., Ylinen, A., Penttonen, M., and Buzsáki, G. (1994). Inhibitory CA1-CA3-hilar region feedback in the hippocampus. *Science* *265*, 1722–1724.
- Snyder, J.S., Soumier, A., Brewer, M., Pickel, J., and Cameron, H.A. (2011). Adult hippocampal neurogenesis buffers stress responses and depressive behaviour. *Nature* *476*, 458–461.
- Tashiro, A., Sandler, V.M., Toni, N., Zhao, C., and Gage, F.H. (2006). NMDA-receptor-mediated, cell-specific integration of new neurons in adult dentate gyrus. *Nature* *442*, 929–933.
- Tashiro, A., Makino, H., and Gage, F.H. (2007). Experience-specific functional modification of the dentate gyrus through adult neurogenesis: a critical period during an immature stage. *J. Neurosci.* *27*, 3252–3259.
- Ugolini, G. (2011). Rabies virus as a transneuronal tracer of neuronal connections. *Adv. Virus Res.* *79*, 165–202.
- van Praag, H., Kempermann, G., and Gage, F.H. (1999). Running increases cell proliferation and neurogenesis in the adult mouse dentate gyrus. *Nat. Neurosci.* *2*, 266–270.
- van Praag, H., Kempermann, G., and Gage, F.H. (2000). Neural consequences of environmental enrichment. *Nat. Rev. Neurosci.* *1*, 191–198.
- van Praag, H., Schinder, A.F., Christie, B.R., Toni, N., Palmer, T.D., and Gage, F.H. (2002). Functional neurogenesis in the adult hippocampus. *Nature* *415*, 1030–1034.
- Vivar, C., Potter, M.C., Choi, J., Lee, J.Y., Stringer, T.P., Callaway, E.M., Gage, F.H., Suh, H., and van Praag, H. (2012). Monosynaptic inputs to new neurons in the dentate gyrus. *Nat. Commun.* *3*, 1107.
- Wickersham, I.R., Lyon, D.C., Barnard, R.J., Mori, T., Finke, S., Conzelmann, K.K., Young, J.A., and Callaway, E.M. (2007). Monosynaptic restriction of transsynaptic tracing from single, genetically targeted neurons. *Neuron* *53*, 639–647.
- Zhao, C., Teng, E.M., Summers, R.G., Jr., Ming, G.L., and Gage, F.H. (2006). Distinct morphological stages of dentate granule neuron maturation in the adult mouse hippocampus. *J. Neurosci.* *26*, 3–11.